ENGINEERING Information Technology & Electronic Engineering
https://www.academax.com/EITEE; https://www.engineering.org.cn
https://ieeexplore.ieee.org/xpl/RecentIssue.jsp?punumber=11344065
E-mail: eng.itee@zju.edu.cn

Supplementary materials for

Liya HU, Bo BAI, Juntao YANG, Mingxuan SONG, Youwei LI, Dandan LIU, Zhenhai LI, Yirou LIU, Guowei LI, 2026. High-throughput estimation of aboveground peanut biomass with optimized spectral–textural features from unmanned aerial vehicle multispectral imagery. *ENGINEERING Inform Technol Electron Eng*, 26(8):260108.
https://doi.org/10.1631/ENG.ITEE.2026.0108

1 Methodology

Table S1 Vegetation Indices

VIs	Acronym	Formula
Normalized Difference Vegetation Index	NDVI	$\frac{\rho_{NIR}-\rho_{Red}}{\rho_{NIR}+\rho_{Red}}$
Normalized Difference Water Index	NDWI	$\frac{\rho_{Green}-\rho_{NIR}}{\rho_{Green}+\rho_{NIR}}$
Green Normalized Difference Vegetation Index	GNDVI	$\frac{\rho_{NIR}-\rho_{Green}}{\rho_{NIR}+\rho_{Green}}$
Soil-Adjusted Vegetation Index	SAVI	$\frac{\rho_{NIR}-\rho_{Red}}{\rho_{NIR}+\rho_{Red}+L}(1+L)$; Default value L=0.5
Normalized Difference Red-Edge Indices	NDRE	$\frac{\rho_{NIR}-\rho_{Red\text{-}Edge}}{\rho_{NIR}+\rho_{Red\text{-}Edge}}$
Modified Soil Adjusted Vegetation Index	MSAVI	$\frac{2\rho_{NIR}+1-\sqrt{(2\rho_{NIR}+1)^2-8(\rho_{NIR}-R)}}{2}$
Ratio Vegetation Index	RVI	$\frac{\rho_{NIR}}{\rho_{Red}}$
Difference Vegetation Index	DVI	$\rho_{NIR}-\rho_{Red}$
Near-infrared Reflectance of Vegetation	NIRv	$NDVI\times\rho_{NIR}$
Optimized Soil Adjusted Vegetation Index	OSAVI	$\frac{1.16*(\rho_{NIR}-\rho_{Red})}{\rho_{NIR}+\rho_{Red}+X}$;Default value X=0.16

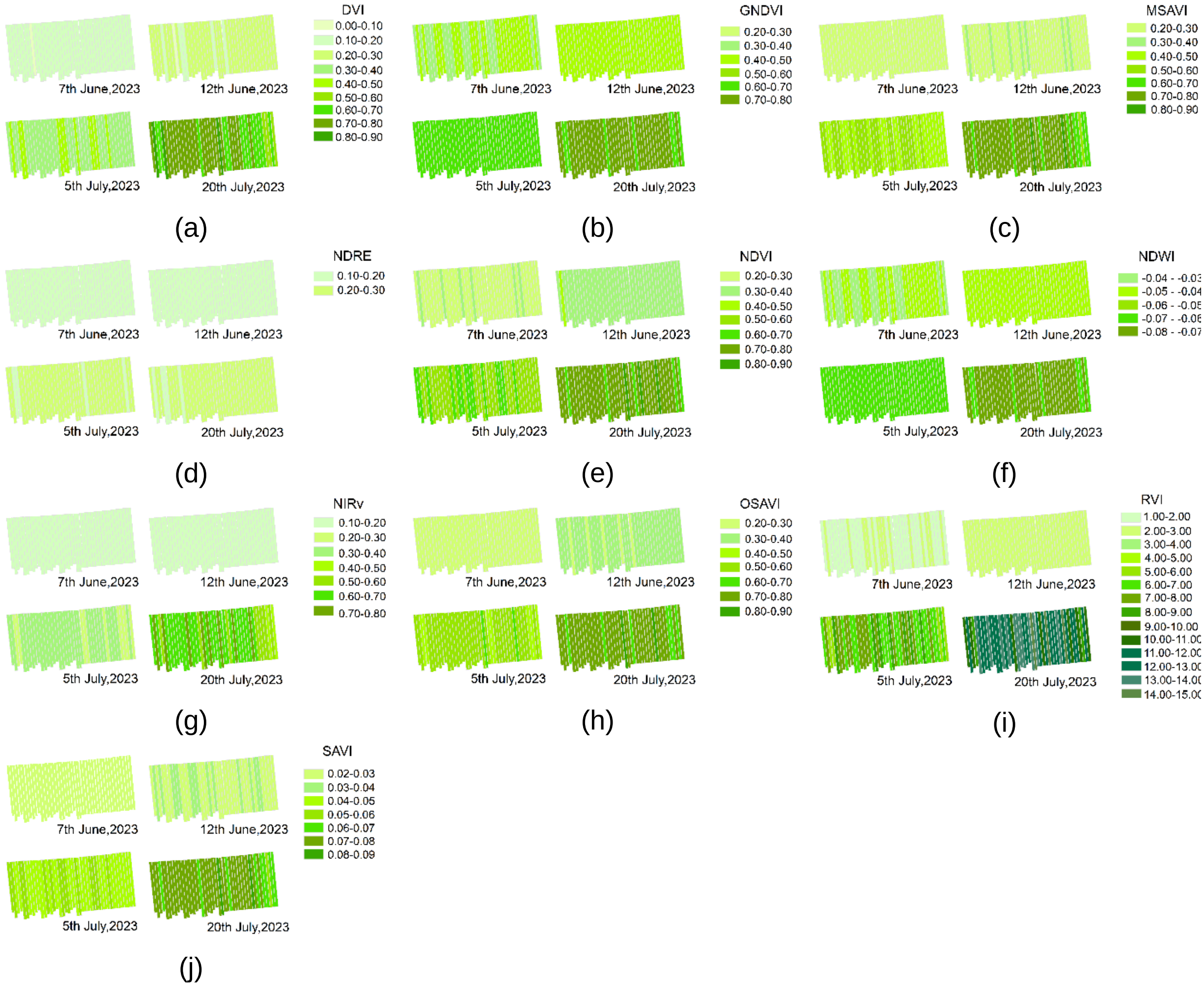

Fig. S1 Representative distributions of vegetation indices across the four peanut growth stages: (a) DVI; (b) GNDVI; (c) MSAVI; (d) NDRE; (e) NDVI; (f) NDWI; (g) NIRv; (h) OSAVI; (i) RVI; (j) SAVI

Table S2 GLCM Texture Features

Texture Metrics	Formula
Mean	$\mu_x = \sum_{i=0}^{N-1}\sum_{j=0}^{N-1} iP(i-j)$
Variance	$\sum_{i=0}^{N-1}\sum_{j=0}^{N-1}(i-\mu_x)^2\, P(i,j)$
Homogeneity	$\sum_{i=0}^{N-1}\sum_{j=0}^{N-1}\frac{P(i,j)}{1+(i-j)^2}$
Contrast	$\sum_{i=0}^{N-1}\sum_{j=0}^{N-1}(i-j)^2\, P(i,j)$
Dissimilarity	$\sum_{i=0}^{N-1}\sum_{j=0}^{N-1}\lvert i-j\rvert\, P(i,j)$
Entropy	$\sum_{i=0}^{N-1}\sum_{j=0}^{N-1} P(i,j)lnP(i,j)$
Energy	$\sqrt{\sum_{i=0}^{N-1}\sum_{j=0}^{N-1} P(i,j)^2}$
Correlation	$\sum_{i=0}^{N-1}\sum_{j=0}^{N-1}\frac{(i-\mu_x)(j-\mu_y)P(i,j)}{\sigma^x\sigma^y}$

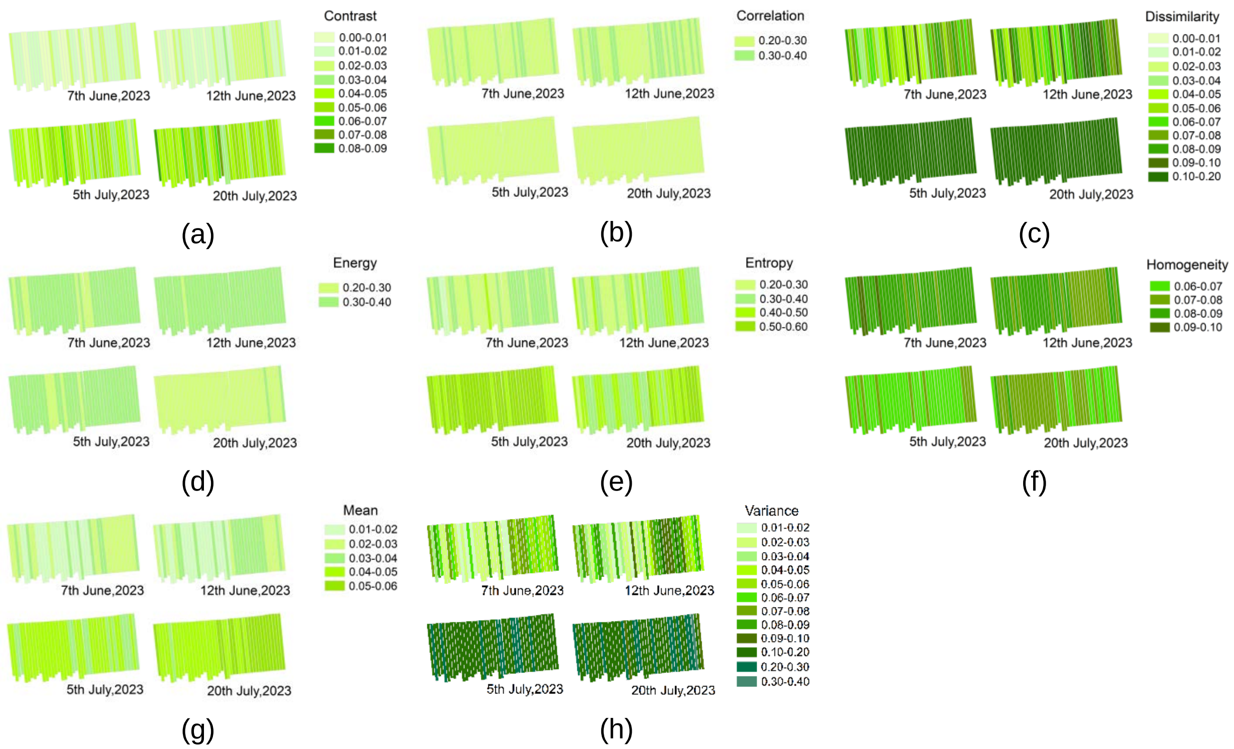

Fig. S2 Temporal evolution of eight TFs from June 7 to July 20: (a) contrast; (b) correlation; (c) dissimilarity; (d) energy; (e) entropy; (f) homogeneity; (g) mean; (h) variance

2 Experiment and analysis

Table S3 GLCM combinations with the best performance in the NIR band across 6 models

Model	Window	Direction	Gray level	R^2	*RMSE*	Mean of R^2	Mean of RMSE
RFR	7×7	45°	16	0.862	0.050	0.854	0.051
	7×7	45°	64	0.860	0.051		
	5×5	45°	32	0.850	0.052		
	5×5	90°	64	0.850	0.053		
	5×5	0°	16	0.848	0.053		
DTR	5×5	0°	32	0.801	0.060	0.766	0.066
	5×5	90°	32	0.780	0.064		
	7×7	90°	16	0.773	0.065		
	3×3	135°	32	0.741	0.069		
	3×3	135°	64	0.736	0.070		
MLR	5×5	90°	32	0.848	0.053	0.840	0.054
	7×7	135°	32	0.842	0.054		
	5×5	90°	64	0.839	0.054		
	7×7	45°	32	0.837	0.055		
	5×5	90°	16	0.836	0.055		
PLSR	5×5	45°	16	0.846	0.053	0.839	0.054
	5×5	135°	16	0.842	0.054		
	7×7	45°	32	0.839	0.054		
	7×7	0°	32	0.837	0.055		
	7×7	90°	32	0.830	0.056		
RR	5×5	45°	16	0.861	0.051	0.854	0.052
	5×5	135°	16	0.861	0.051		
	7×7	45°	32	0.850	0.053		
	5×5	0°	32	0.849	0.053		
	5×5	90°	32	0.849	0.053		
SVR	5×5	135°	16	0.672	0.078	0.656	0.080
	5×5	45°	16	0.664	0.079		
	3×3	45°	16	0.653	0.079		
	3×3	0°	16	0.645	0.081		
	5×5	0°	32	0.644	0.081		

3 Discussion

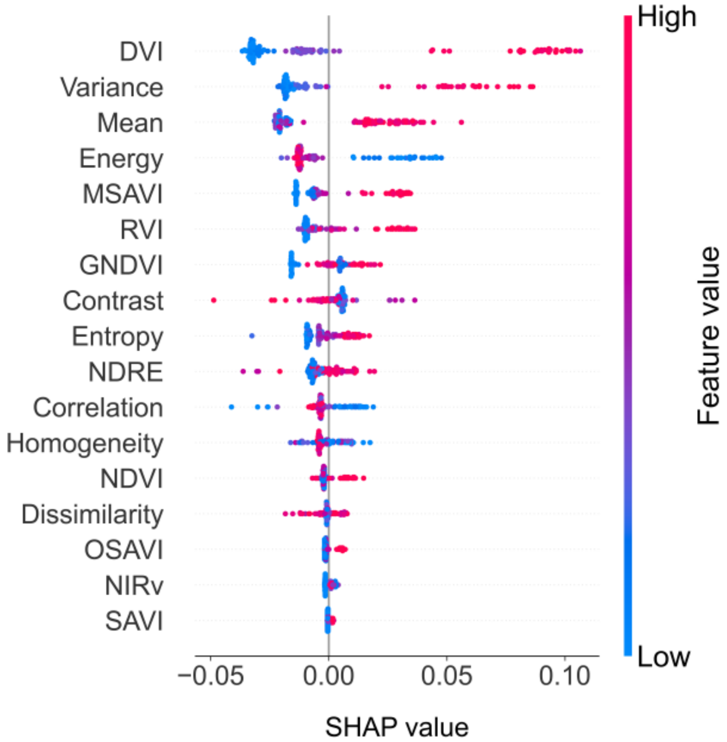

Fig. S3 Ranking of feature contributions for peanut AGB prediction based on XGBoost-SHAP analysis

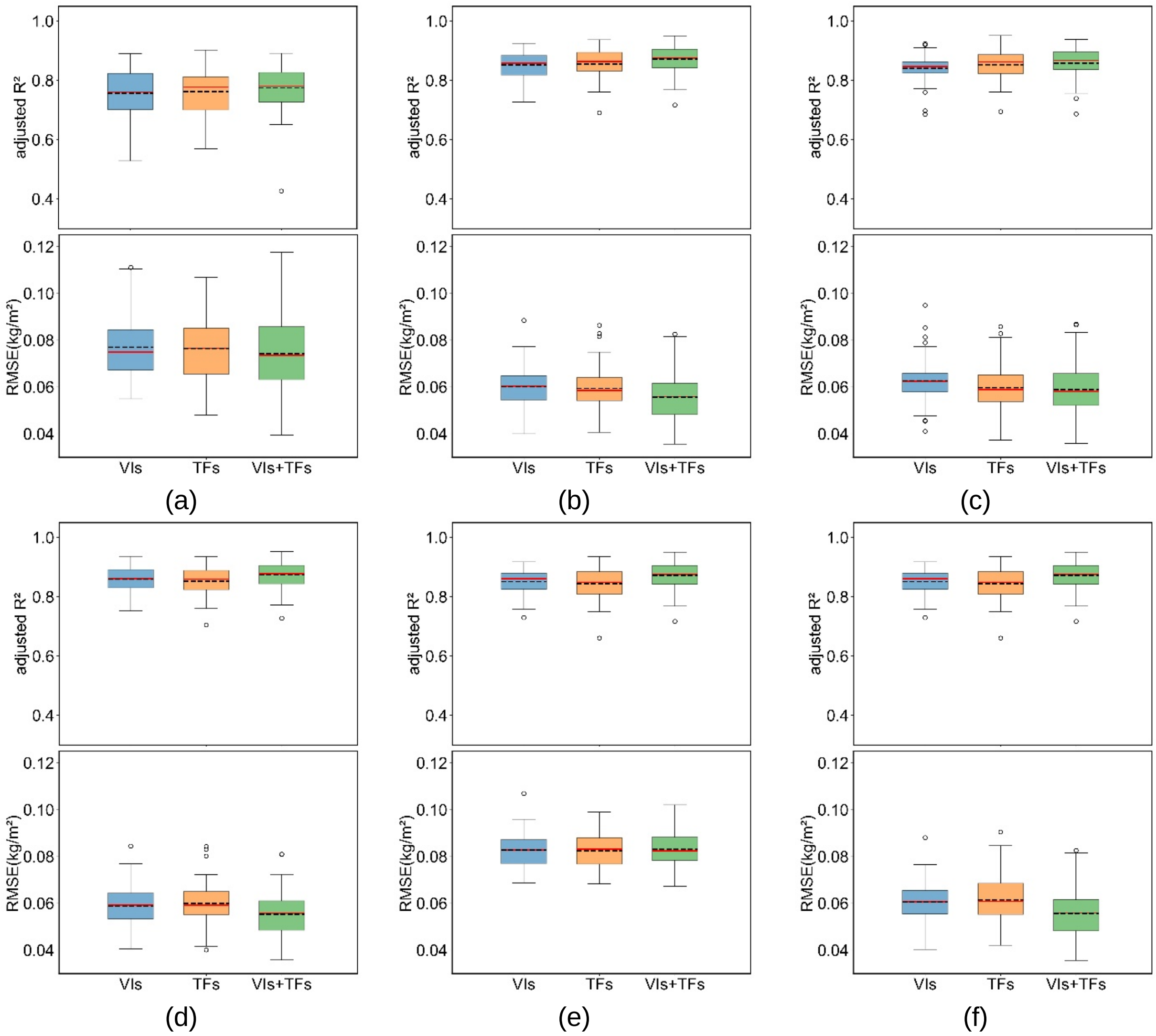

Fig. S4 Distributions of validation adjusted R^2 and RMSE obtained from 50 repeated random using the nine-VI feature set, eight-TF feature set, and XGBoost-SHAP-selected five-feature set: (a) Performance of the DTR model; (b) Performance of the PLSR model; (c) Performance of the RFR model; (d) Performance of the RR model; (e) Performance of the SVR model; (f) Performance of the MLR model was evaluated over 50 random runs